Detection of light speed anisotropy and Aether wind speed using a small, portable detector

Abstract

This paper describes an experiment using a small, cheap, portable Aether wind detector that can be made for just a few hundred dollars and can successfully detect the light speed anisotropy in the Earth's reference frame and determine its magnitude and direction.

In earlier work done by other researchers such as Torr and Kolen (1981) [1], Krisher (1990) [2], De Witte (1991) [3] and NASA (2008) [4], the motion of the Earth through the Aether was detected as an anisotropy in the propagation speed of light in the Earth's reference frame. All experiments determined very similar speed and direction of the Aether wind, with a sidereal (galactic) origin of about 486 km/s in the direction RA = 4.29 h, Dec = -75.0 Deg [5]. However, these experiments all require large and expensive detectors, often involving kilometres of coaxial cable or optic fibre or space craft in order to detect the light speed anisotropy.

This paper describes an experiment using a small, cheap, portable Aether wind detector that can be made for just a few hundred dollars and can successfully detect the light speed anisotropy in the Earth's reference frame and determine its magnitude and direction.

The detector comprises 10 identical, double-sided PCBs with a total length of 1820.4 meters of copper track which loops back and forth along the length of the PCB substrate. The PCB dielectric material is FR4 which has a dielectric constant of 4.6, giving the signal path an effective refractive index of 2.14476. The PCBs are constructed with internal ground planes such that the track is a microstrip with impedance of 50 Ohms. All PCBs are connected together in serial to form one long track. A Vector Network Analyser (also with impedance of 50 Ohms) is connected to each end of the detectors copper track such that it emits a sweeping RF signal into one end of the track and measures the properties of the detector circuit, including the overall phase delay. It is variations in this detected phase delay (between different orientations of the detector: North/South or East/West) which reveals the light speed anisotropy in the Earth's reference frame and thus the existence of the Aether wind and Absolute reference frame. The entire detector and VNA were housed inside a steel box to prevent external magnetic and/or RF signal interference during the collection of the data sets.

A series of 10 sets of results data in each of the two orientations, North/South and East/West, were collected from the detector over the space of a few minutes on 31/12/2022 at 7.30am in Melbourne, Australia. The first set of 10 readings was taken with the detector aligned in the North/South direction, then the detector was carefully repositioned to point East/West and the second set of 10 readings taken. The VNA performed a sweep over the frequency range of 6.0 MHZ to 12.0 MHz in 60KHz steps. The 10 sets of data were then averaged to produce a final results data set (Appendix A). This set of data was then averaged over all swept frequencies to obtain a final phase timing difference between detector orientations (North/South and East/West).

This timing value was then input into the mathematical model (based on the theoretical calculations for this type of detector [6]) and the modelled Aether wind speed adjusted slightly from the expected value of 486 km/s (based on other experimenters' findings) such that the timing value in the model matched that found by experiment, to obtain a final corresponding detected Aether wind speed of 486.850 km/s. This finding is in excellent agreement with the finding of other researchers.

Experimental Setup

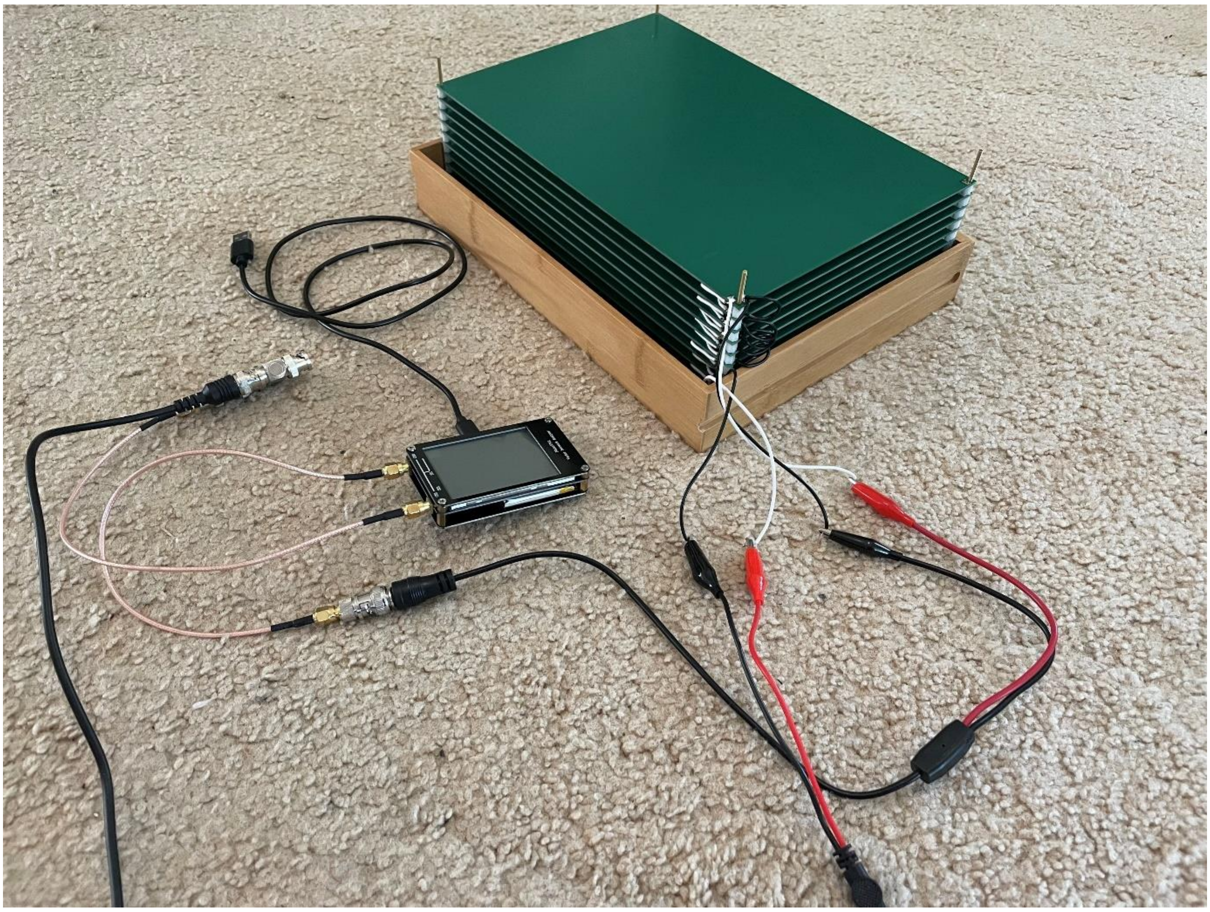

Image 1: The full experimental setup (except for the PC that collects the data and the steel enclosure)

Image 2: The stack up of 10 double-sided PCBs that have the looping copper track etched into it. All PCBs are connected in series.

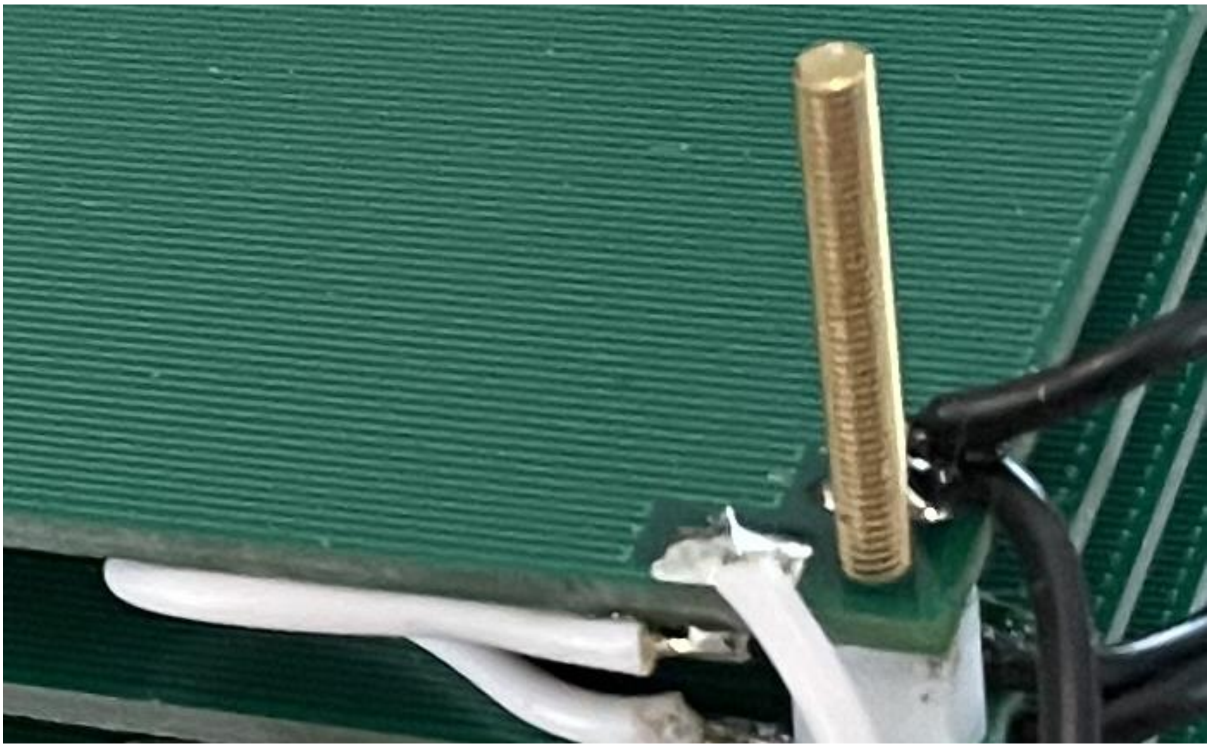

Image 3: A close up view of the etched copper track on the top PCB.

Image 4: The steel enclosure box that houses the PCB stack, Vector Network Analyser and cables, to prevent external magnetic and RF interference with the recorded results data.

Results

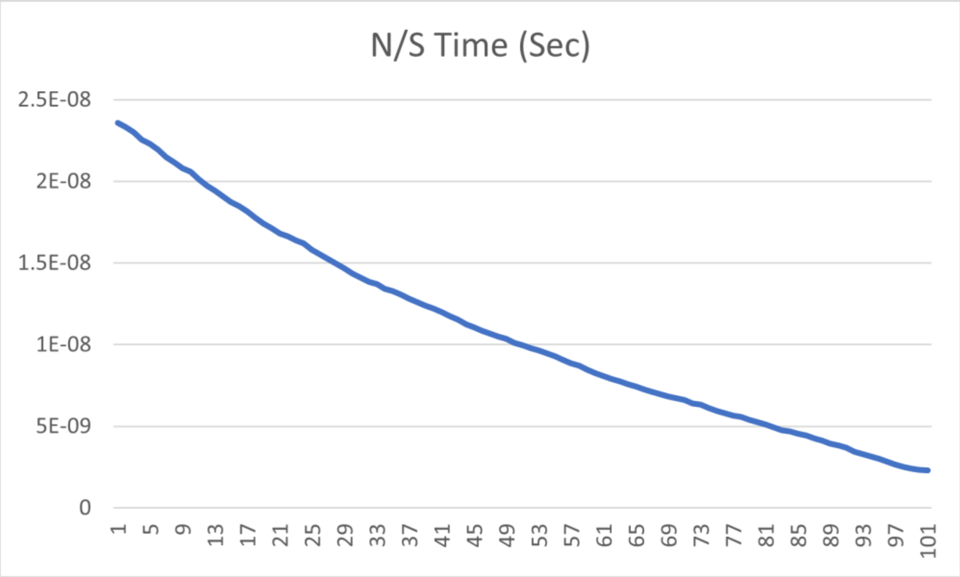

Figure 1: The Phase timing graph versus frequency graph for the North/South direction.

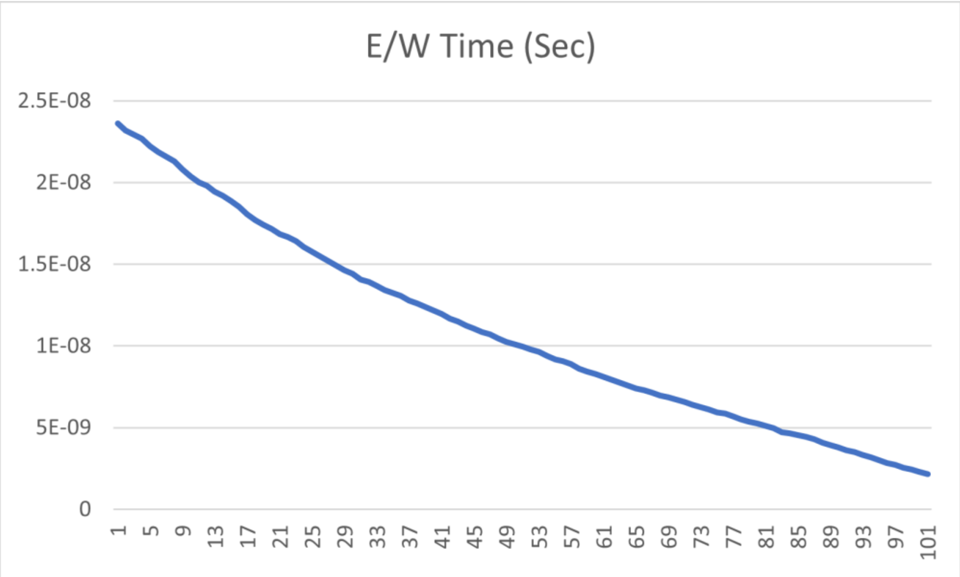

Figure 2: The Phase timing graph versus frequency graph for the East/West direction.

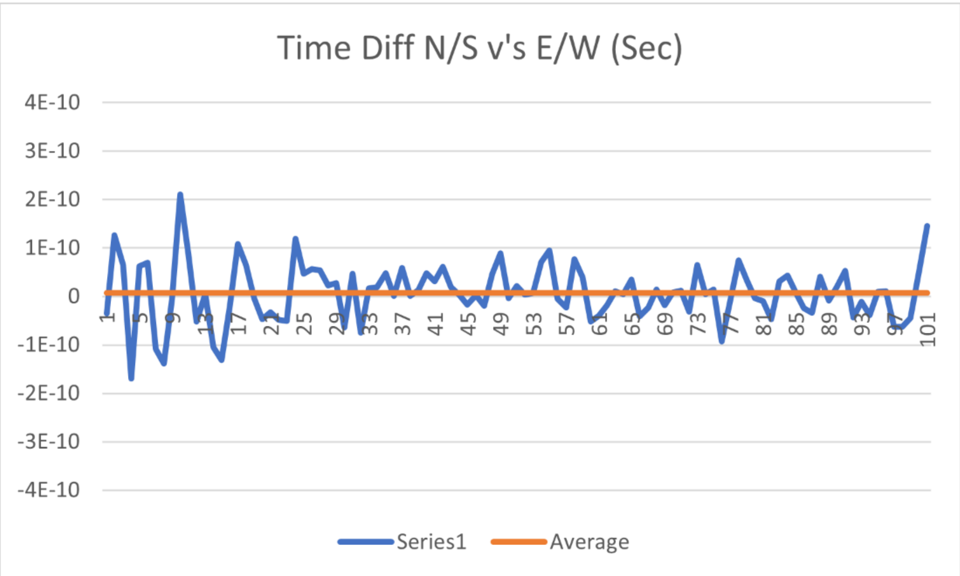

Figure 3: The Phase timing difference graph versus frequency graph for the North/South versus East/West directions.

Appendix A: The collected data set for each scanned frequency. Each row comprises averaged data from 10 individual measurements at each frequency. The final figure highlighted in yellow shows the overall average timing difference (across all scanned frequencies) between the two detector orientations: North/South and East/West.

Frequency (Hz)	Phase Diff N/S v's E/W		N/S Time (Sec)	E/W Time (Sec)	Time Diff N/S v's E/W (Sec)
6.00000000000E+6	-0.074870468		2.35931E-08	2.36278E-08	-3.46623E-11
6.06000000000E+6	0.276172872		2.33205E-08	2.31939E-08	1.26592E-10
6.12000000000E+6	0.142204432		2.30071E-08	2.29426E-08	6.45445E-11
6.18000000000E+6	-0.376888258		2.25368E-08	2.27062E-08	-1.69403E-10
6.24000000000E+6	0.139860355		2.23029E-08	2.22407E-08	6.22598E-11
6.30000000000E+6	0.157643259		2.19529E-08	2.18834E-08	6.95076E-11
6.36000000000E+6	-0.247571428		2.14796E-08	2.15877E-08	-1.08129E-10
6.42000000000E+6	-0.319557878		2.11643E-08	2.13026E-08	-1.38265E-10
6.48000000000E+6	-0.012722661		2.08093E-08	2.08148E-08	-5.45382E-12
6.54000000000E+6	0.495524544		2.05925E-08	2.0382E-08	2.10467E-10
6.60000000000E+6	0.209477757		2.01082E-08	2.002E-08	8.8164E-11
6.66000000000E+6	-0.125141173		1.97404E-08	1.97926E-08	-5.21943E-11
6.72000000000E+6	0.011468638		1.94402E-08	1.94355E-08	4.74067E-12
6.78000000000E+6	-0.255435331		1.91033E-08	1.92079E-08	-1.04652E-10
6.84000000000E+6	-0.323638726		1.87434E-08	1.88749E-08	-1.31432E-10
6.90000000000E+6	-0.05412745		1.84789E-08	1.85007E-08	-2.17904E-11
6.96000000000E+6	0.270968324		1.81684E-08	1.80603E-08	1.08145E-10
7.02000000000E+6	0.163443227		1.77763E-08	1.77116E-08	6.46736E-11
7.08000000000E+6	-0.008633027		1.73963E-08	1.73997E-08	-3.38709E-12
7.14000000000E+6	-0.120009981		1.71291E-08	1.71758E-08	-4.66892E-11
7.20000000000E+6	-0.084076404		1.68141E-08	1.68466E-08	-3.24369E-11
7.26000000000E+6	-0.125317758		1.66165E-08	1.66644E-08	-4.79483E-11
7.32000000000E+6	-0.133687423		1.63756E-08	1.64264E-08	-5.07314E-11
7.38000000000E+6	0.314980972		1.61931E-08	1.60745E-08	1.18557E-10
7.44000000000E+6	0.126881987		1.58236E-08	1.57763E-08	4.73723E-11
7.50000000000E+6	0.153052939		1.55375E-08	1.54808E-08	5.66863E-11
7.56000000000E+6	0.146333313		1.52553E-08	1.52015E-08	5.37674E-11
7.62000000000E+6	0.06094673		1.49505E-08	1.49283E-08	2.22174E-11
7.68000000000E+6	0.077843449		1.46664E-08	1.46382E-08	2.81552E-11

7.74000000000E+6	- 0.176946867		1.43427E-08	1.44062E-08	-6.35038E-11
7.80000000000E+6	0.132234173		1.41121E-08	1.4065E-08	4.70919E-11
7.86000000000E+6	- 0.209735021		1.38605E-08	1.39346E-08	-7.41218E-11
7.92000000000E+6	0.046472795		1.37002E-08	1.3684E-08	1.62994E-11
7.98000000000E+6	0.053509851		1.343E-08	1.34114E-08	1.86264E-11
8.04000000000E+6	0.137970581		1.32789E-08	1.32312E-08	4.76681E-11
8.10000000000E+6	0.004424843		1.30513E-08	1.30498E-08	1.51744E-12
8.16000000000E+6	0.171637946		1.28289E-08	1.27704E-08	5.8428E-11
8.22000000000E+6	0.00346207		1.26048E-08	1.26037E-08	1.16993E-12
8.28000000000E+6	0.039225386		1.24037E-08	1.23905E-08	1.31593E-11
8.34000000000E+6	0.144216603		1.22216E-08	1.21736E-08	4.80338E-11
8.40000000000E+6	0.093554683		1.19914E-08	1.19605E-08	3.09374E-11
8.46000000000E+6	0.186831586		1.17503E-08	1.1689E-08	6.13448E-11
8.52000000000E+6	0.057470398		1.15213E-08	1.15025E-08	1.87371E-11
8.58000000000E+6	0.011179287		1.12464E-08	1.12428E-08	3.6193E-12
8.64000000000E+6	- 0.052459407		1.10514E-08	1.10682E-08	-1.68658E-11
8.70000000000E+6	0.00793256		1.08638E-08	1.08612E-08	2.53275E-12
8.76000000000E+6	- 0.059662183		1.0694E-08	1.0713E-08	-1.89188E-11
8.82000000000E+6	0.149583721		1.04954E-08	1.04483E-08	4.711E-11
8.88000000000E+6	0.283603767		1.03406E-08	1.02519E-08	8.87149E-11
8.94000000000E+6	-0.01119795		1.00991E-08	1.01025E-08	-3.47935E-12
9.00000000000E+6	0.068168685		9.97604E-09	9.955E-09	2.10397E-11
9.06000000000E+6	0.011162371		9.79833E-09	9.7949E-09	3.42236E-12
9.12000000000E+6	0.024098693		9.64657E-09	9.63923E-09	7.34E-12
9.18000000000E+6	0.232612947		9.46262E-09	9.39223E-09	7.03864E-11
9.24000000000E+6	0.314818491		9.28097E-09	9.18633E-09	9.46424E-11
9.30000000000E+6	- 0.016087598		9.0764E-09	9.08121E-09	-4.80514E-12
9.36000000000E+6	-0.07848332		8.85611E-09	8.8794E-09	-2.32916E-11
9.42000000000E+6	0.258843862		8.69918E-09	8.62285E-09	7.63281E-11
9.48000000000E+6	0.136267242		8.4712E-09	8.43127E-09	3.99283E-11
9.54000000000E+6	- 0.177016916		8.24864E-09	8.30018E-09	-5.15423E-11
9.60000000000E+6	- 0.135574329		8.0799E-09	8.11913E-09	-3.92287E-11
9.66000000000E+6	- 0.063218389		7.90525E-09	7.92343E-09	-1.81787E-11
9.72000000000E+6	0.038110459		7.75272E-09	7.74183E-09	1.08912E-11
9.78000000000E+6	0.015718482		7.57159E-09	7.56713E-09	4.46446E-12
9.84000000000E+6	0.124502922		7.437E-09	7.40186E-09	3.51465E-11
9.90000000000E+6	- 0.144961919		7.26415E-09	7.30483E-09	-4.06739E-11
9.96000000000E+6	- 0.081710969		7.12626E-09	7.14904E-09	-2.27886E-11
1.00200000000E+7	0.051979119		6.98286E-09	6.96845E-09	1.44098E-11
1.00800000000E+7	-0.0674784		6.82879E-09	6.84738E-09	-1.85952E-11
1.01400000000E+7	0.030476769		6.71136E-09	6.70302E-09	8.34888E-12
1.02000000000E+7	0.043006309		6.5949E-09	6.58319E-09	1.1712E-11
1.02600000000E+7	- 0.113943965		6.38137E-09	6.41221E-09	-3.0849E-11

1.03200000000E+7	0.240606143		6.31826E-09	6.25349E-09	6.47626E-11
1.03800000000E+7	0.01581537		6.12846E-09	6.12423E-09	4.23233E-12
1.04400000000E+7	0.054273272		5.94078E-09	5.92634E-09	1.44405E-11
1.05000000000E+7	-0.352046337		5.78546E-09	5.87859E-09	-9.3134E-11
1.05600000000E+7	-0.044157983		5.66725E-09	5.67887E-09	-1.16156E-11
1.06200000000E+7	0.285813706		5.5755E-09	5.50074E-09	7.47577E-11
1.06800000000E+7	0.127547652		5.40585E-09	5.37268E-09	3.31741E-11
1.07400000000E+7	-0.015653414		5.24393E-09	5.24798E-09	-4.04858E-12
1.08000000000E+7	-0.03650872		5.11838E-09	5.12777E-09	-9.3901E-12
1.08600000000E+7	-0.183068957		4.92822E-09	4.97504E-09	-4.68255E-11
1.09200000000E+7	0.120453715		4.76645E-09	4.73581E-09	3.06404E-11
1.09800000000E+7	0.168838966		4.69999E-09	4.65727E-09	4.27138E-11
1.10400000000E+7	0.034466656		4.54104E-09	4.53236E-09	8.67217E-12
1.11000000000E+7	-0.098072965		4.42113E-09	4.44568E-09	-2.45428E-11
1.11600000000E+7	-0.137762851		4.26189E-09	4.29618E-09	-3.42898E-11
1.12200000000E+7	0.163265601		4.13154E-09	4.09112E-09	4.04203E-11
1.12800000000E+7	-0.036778738		3.93049E-09	3.93955E-09	-9.05702E-12
1.13400000000E+7	0.084568325		3.82686E-09	3.80615E-09	2.07153E-11
1.14000000000E+7	0.214793012		3.68019E-09	3.62785E-09	5.23375E-11
1.14600000000E+7	-0.181551873		3.44844E-09	3.49245E-09	-4.40062E-11
1.15200000000E+7	-0.044504209		3.30646E-09	3.31719E-09	-1.07311E-11
1.15800000000E+7	-0.160619835		3.14642E-09	3.18495E-09	-3.8529E-11
1.16400000000E+7	0.038497138		3.01447E-09	3.00528E-09	9.18698E-12
1.17000000000E+7	0.047126493		2.84837E-09	2.83719E-09	1.11886E-11
1.17600000000E+7	-0.264614285		2.66411E-09	2.72661E-09	-6.25034E-11
1.18200000000E+7	-0.268538487		2.49572E-09	2.55882E-09	-6.31083E-11
1.18800000000E+7	-0.189555265		2.39062E-09	2.43494E-09	-4.43218E-11
1.19400000000E+7	0.229208578		2.34683E-09	2.2935E-09	5.33242E-11
1.20000000000E+7	0.630462999		2.29012E-09	2.14418E-09	1.45941E-10
Averages	0.024120279				7.57709E-12

Appendix B: The Azimuth/Altitude of the expected Aether wind at 7:30am on 31/12/2022 in Melbourne, Australia at the location where the experiment was conducted.

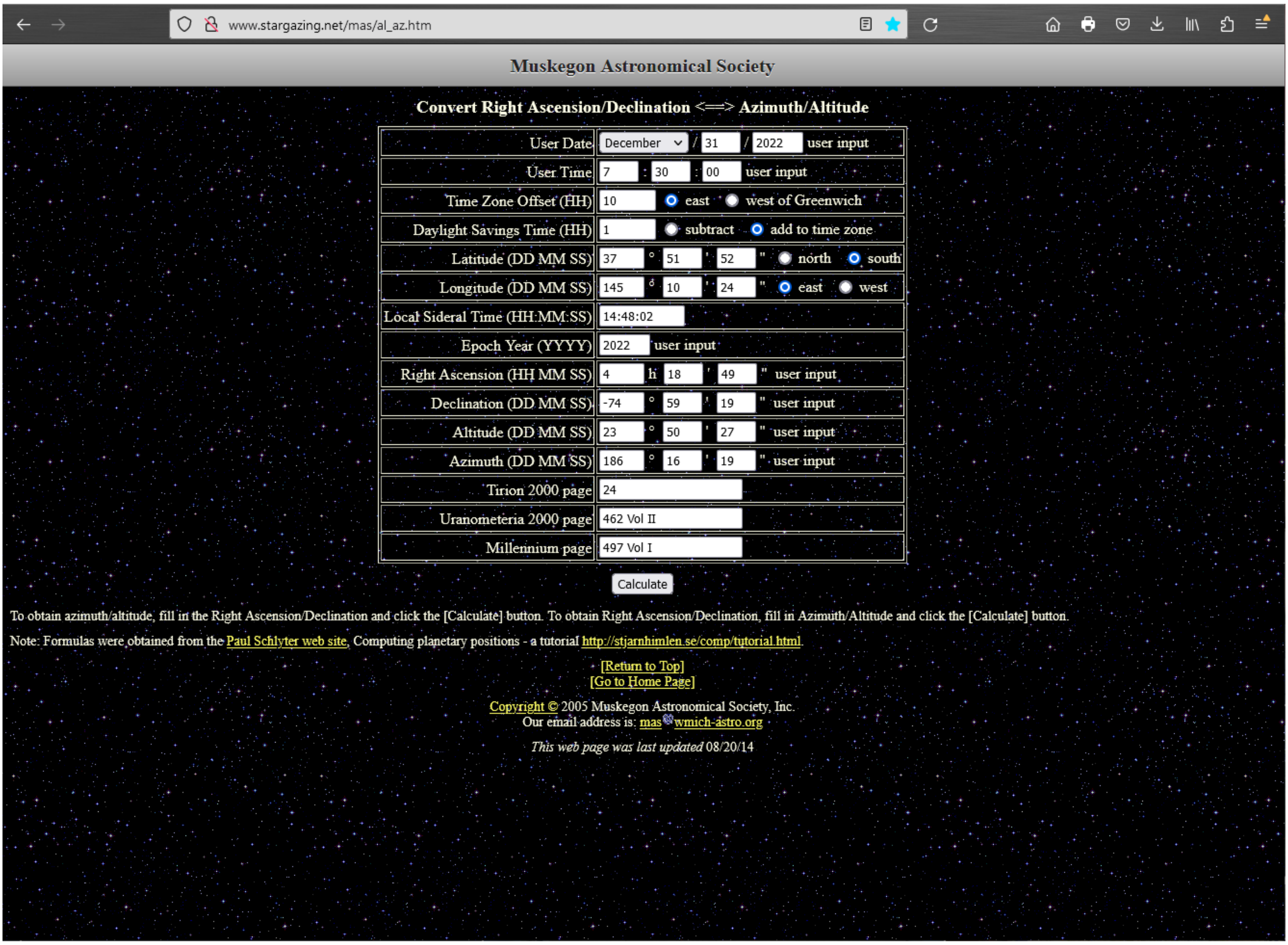

Appendix C: The mathematical modelling for the detector. The model calculates the expected theoretical timing difference between North/South and East/West orientations of the detector [6], given a particular Aether wind speed and direction.

>

[*animate*, *animate3d*, *animatecurve*, *arrow*, *changecoords*, *complexplot*, *complexplot3d*, *conformal*, *conformal3d*, *contourplot*, *contourplot3d*, *coordplot*, *coordplot3d*, *densityplot*, *display*, *dualaxisplot*, *fieldplot*, *fieldplot3d*, *gradplot*, *gradplot3d*, *implicitplot*, *implicitplot3d*, *inequal*, *interactive*, *interactiveparams*, *intersectplot*, *listcontplot*, *listcontplot3d*, *listdensityplot*, *listplot*, *listplot3d*, *loglogplot*, *logplot*, *matrixplot*, *multiple*, *odeplot*, *pareto*, *plotcompare*, *pointplot*, *pointplot3d*, *polarplot*, *polygonplot*, *polygonplot3d*, *polyhedra_supported*, *polyhedraplot*, *rootlocus*, *semilogplot*, *setcolors*, *setoptions*, *setoptions3d*, *spacecurve*, *sparsematrixplot*, *surfdata*, *textplot*, *textplot3d*, *tubeplot*]

$$Digits := 50$$

$$c := 299792458$$

$$f := 9.0\ 10^{6}$$

$$\lambda := 33.310273111111111111111111111111111111111111111111$$

$$FullLoopsPerPCBside := 146$$

$$MediumLoopsPerPCBside := 10$$

$$ShortLoopsPerPCBside := 3.5$$

$$NumberOfPCBs := 10$$

$$NumberOfSidesToPCB := 2$$

$$TrackWidth := 0.0003$$

$$InterTrackSpacing := 0.00065$$

$$NumberOfFullLoops := 2920$$

$$NumberOfMediumLoops := 70.0$$

$$NumberOfShortLoops := 70.0$$

$$SingleFullLoopLength := 0.298$$

$$SingleMediumLoopLength := 0.288$$

$$SingleShortLoopLength := 0.284$$

$$DielectricConstant := 4.6$$

$$TotalArmLength := 910.2000$$

$$TotalPCBwidth := 0.199375$$

$$Altitude := 0.13244444444444444444444444444444444444444444444444\pi$$

$$Azimuth := 1.0347222222222222222222222222222222222222222222222\pi$$

$$vWind := -486850$$

$$v := -4.4266406953082430979342358815542155505403987394191\ 10^{5}$$

$$n1 := 2.1447610589527216609628319344308569410180423711101$$

$$unitXcomponent := |\cos(\theta)|^2$$

$$unitYcomponent := |\sin(\theta)|^2$$

$$\gamma := 1.0000010901288999948210761694201180661607443602998$$

$$L1 := 1.0000010901288999948210761694201180661607443602998 L$$

$$Eqdt0 := dtDiagonal = \frac{1}{299792458} L\, n + 3.6362786017612927279492138460206385324086431820776\; 10^{-15} L$$

$$L := 910.2000\, |\cos(\theta)|^2$$

$$n := 2.1447610589527216609628319344308569410180423711101$$

$$dtTotalArmLength1a := 0.000006511713206921609852821958436743453537894311146 8444\, |\cos(\theta)|^2$$

$$n := 2.1447610589527216609628319344308569410180423711101$$

$$dtTotalArmLength1b := 0.000006511713206921609852821958436743453537894311146 8444\, |\cos(\theta)|^2$$

$$L := 910.2000\, |\sin(\theta)|^2$$

$$n := 2.1447610589527216609628319344308569410180423711101$$

$$dtTotalArmLength2a := 0.000006511713206921609852821958436743453537894311146 8444\, |\sin(\theta)|^2$$

$$n := 2.1447610589527216609628319344308569410180423711101$$

$$dtTotalArmLength2b := 0.000006511713206921609852821958436743453537894311146 8444\, |\sin(\theta)|^2$$

$$dtPerpendicularArm1 := 0.000013023426413843219705643916873486907075788622293 689\, |\cos(\theta)|^2$$

$$dtPerpendicularArm2 := 0.000013023426413843219705643916873486907075788622293 689\, |\sin(\theta)|^2$$

$$L := L$$

$$n := n$$

$$FractionOfTimeLightIsHeldByMoleculesUp := \frac{n-1}{n}$$

$$TimeLightIsHeldByMoleculesInMovingFrameUp := \frac{1}{299792458} (n - 1) L$$

$TimeLightIsHeldByMoleculesInAetherFrameUp :=$
$3.335644588260122257048495093963031138564347607102910^{-9}$
$(n-1)\, L$

$opticalPathLengthUp :=$
$0.9999989098722883849020406688532957825876878851729 4 L$
$- 4.42664069530824309793423588155421555054039873941 91$
$10^{5}\, dtup$
$+ 0.00147657000794769658502189877600206043463446903 19$
$22\, (n-1)\, L$

$dtupEqn := dtup$
$= 3.33563731570688274253397218169276220613824743107 09$
$10^{-9}\, L$
$- 0.00147656839829781278151241412535942300140866076 73$
$30\, dtup$
$+ 3.34056989564710027296983591293720980330792320776 72$
$10^{-9}\, (n-1)\, L$

$dtup :=$
$-4.92530738697801592134081897417866474357560066421 59$
$10^{-12}\, L$
$+ 3.33564458826012225704849509396303113856434760710 29$
$10^{-9}\, L\, n$

$$FractionOfTimeLightIsHeldByMoleculesDown := \frac{n-1}{n}$$

$TimeLightIsHeldByMoleculesInMovingFrameDown := \frac{1}{299792458}\, (n$
$- 1)\, L$

$TimeLightIsHeldByMoleculesInAetherFrameDown :=$
$3.335644588260122257048495093963031138564347607102910^{-9}$
$(n-1)\, L$

$opticalPathLengthDown :=$
$0.9999989098722883849020406688532957825876878851729 4 L$
$+ 4.42664069530824309793423588155421555054039873941 91$
$10^{5}\, dtdown$
$- 0.00147657000794769658502189877600206043463446903 19$
$22\, (n-1)\, L$

$dtdownEqn := dtdown$
$= 3.33563731570688274253397218169276220613824743107 09$
$10^{-9}\, L$
$+ 0.00147656839829781278151241412535942300140866076 73$
$30\, dtdown$
$+ 3.33071928087314424112715427498885247382077200643 86$
$10^{-9}\, (n-1)\, L$

$$dtdown := 4.9253073869780159213408189741786647435756006643843\ 10^{-12} L + 3.3356445882601222570484950939630311385643476071029\ 10^{-9} L\, n$$

$$L := 910.2000 \left|\sin(\theta)\right|^2$$

$$n := 2.1447610589527216609628319344308569410180423711101$$

$$dtParallelArm1up := 0.0000065072339810003464387255893849995553602338893758 214 \left|\sin(\theta)\right|^2$$

$$n := 2.1447610589527216609628319344308569410180423711101$$

$$dtParallelArm1down := 0.0000065162000105676012189087982118601502015330943992 707 \left|\sin(\theta)\right|^2$$

$$dtParallelArm1 := 0.0000130234339915679476576343875968597055617669837750 92 \left|\sin(\theta)\right|^2$$

$$dtArm1 := 0.0000130234122166451857951130956354715032149005470842 79 \left|\cos(\theta)\right|^2 + 0.00001302341979436165305938663491473802177981823789 6995 \left|\sin(\theta)\right|^2$$

$$L := 910.2000 \left|\cos(\theta)\right|^2$$

$$n := 2.1447610589527216609628319344308569410180423711101$$

$$dtParallelArm2up := 0.0000065072339810003464387255893849995553602338893758 214 \left|\cos(\theta)\right|^2$$

$$n := 2.1447610589527216609628319344308569410180423711101$$

$$dtParallelArm2down := 0.0000065162000105676012189087982118601502015330943992 707 \left|\cos(\theta)\right|^2$$

$$dtParallelArm2 := 0.0000130234339915679476576343875968597055617669837750 92 \left|\cos(\theta)\right|^2$$

$$dtArm2 := 0.0000130234122166451857951130956354715032149005470842 79 \left|\sin(\theta)\right|^2 + 0.00001302341979436165305938663491473802177981823789 6995 \left|\cos(\theta)\right|^2$$

$$L := L$$

$$n := n$$

$TimeDifference :=$

$1.1111111111111111111111111111111111111111111111111110^{-}$
$Shift$

$dt :=$

$-7.5777164672642735392792665185649176908127161 0^{-12}$
$|\cos(\theta)|^2$
$+ 7.5777164672642735392792665185649176908127161 0^{-12}$
$|\sin(\theta)|^2$

$dtEq :=$

$1.1111111111111111111111111111111111111111111111111110^{-}$
$Shift =$
$-7.5777164672642735392792665185649176908127161 0^{-12}$
$|\cos(\theta)|^2$
$+ 7.5777164672642735392792665185649176908127161 0^{-12}$
$|\sin(\theta)|^2$

$FringeShift :=$

$-0.0000681994482053784618535133986670842592173144400($
$001 |\cos(\theta)|^2$
$+ 0.000068199448205378461853513398667084259217314440($
$0001 |\sin(\theta)|^2$

$$plot1a := PLOT(...)$$

$$plot1b := PLOT(...)$$

$$plot3 := PLOT(...)$$

$$plot4 := PLOT(...)$$

$$plot5 := PLOT(...)$$

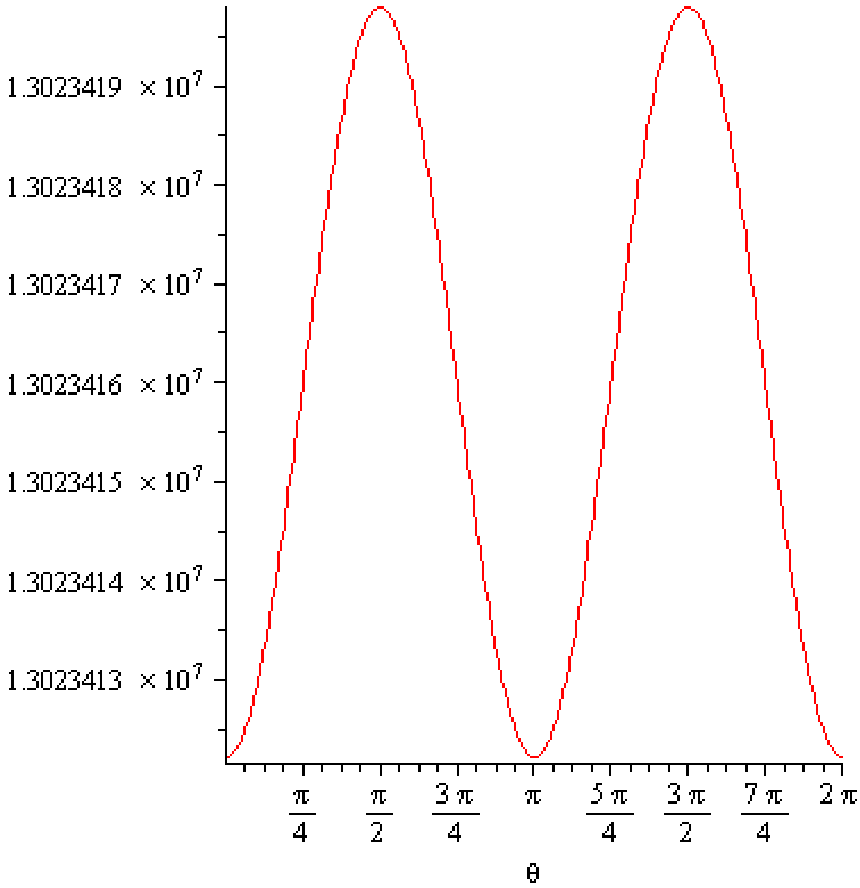

1.3023419 × 10^7
1.3023418 × 10^7
1.3023417 × 10^7
1.3023416 × 10^7
1.3023415 × 10^7
1.3023414 × 10^7
1.3023413 × 10^7
π/4
π/2
3π/4
π
5π/4
3π/2
7π/4
2π
θ

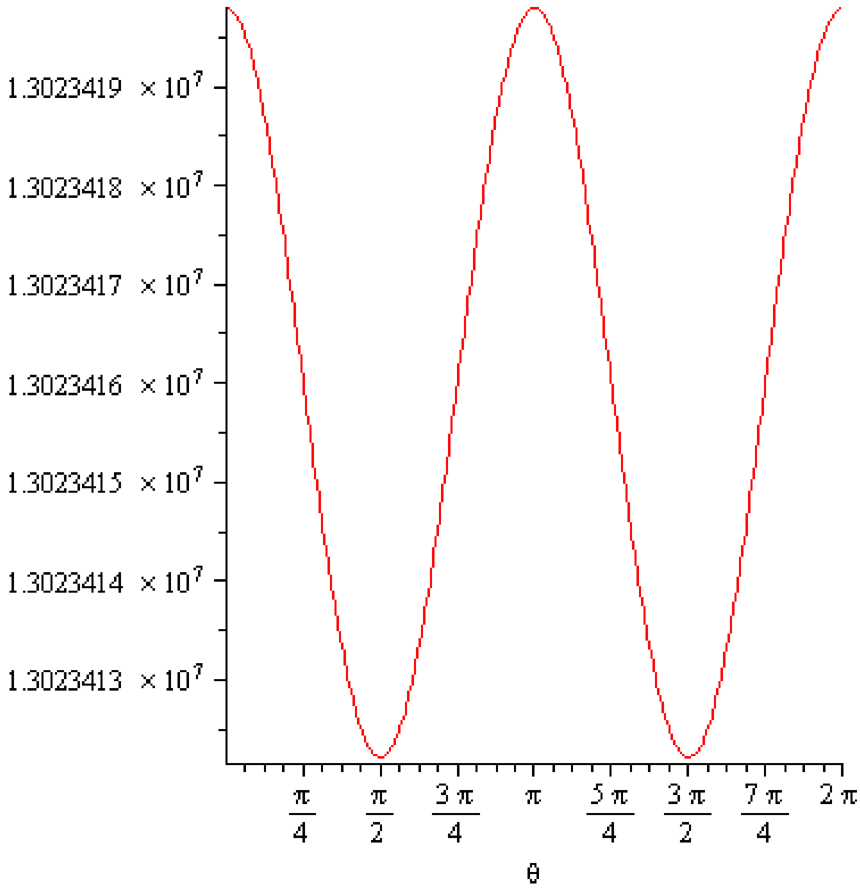

1.3023419 × 10^7
1.3023418 × 10^7
1.3023417 × 10^7
1.3023416 × 10^7
1.3023415 × 10^7
1.3023414 × 10^7
1.3023413 × 10^7
π/4
π/2
3π/4
π
5π/4
3π/2
7π/4
2π
θ

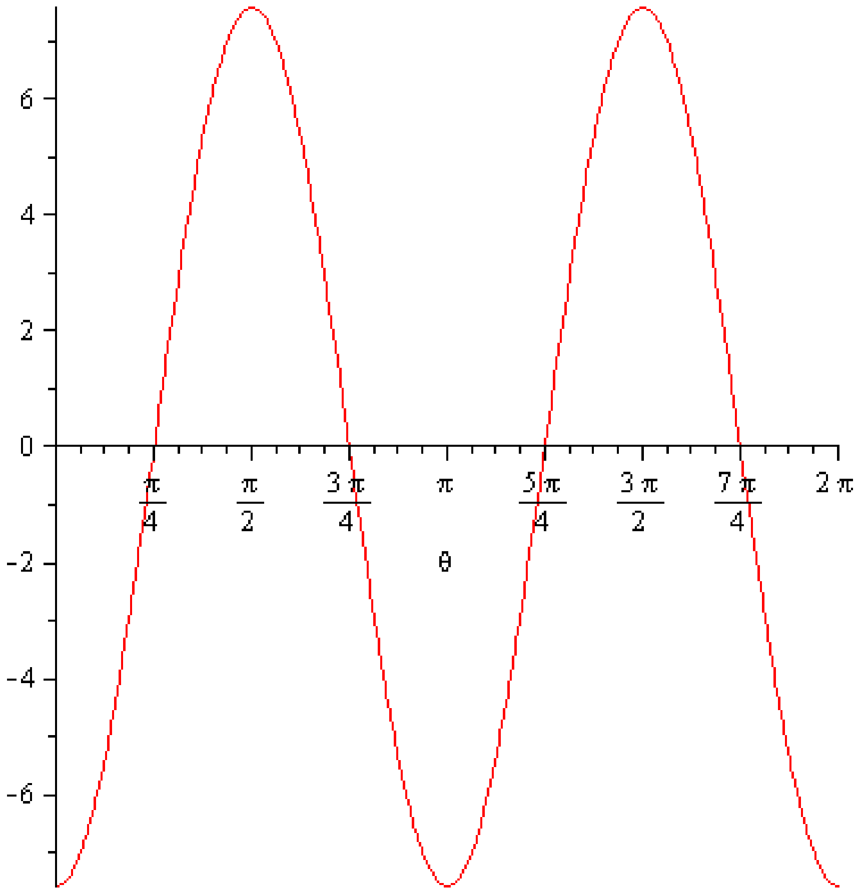
6
4
2
0
-2
-4
-6
π/4
π/2
3π/4
π
5π/4
3π/2
7π/4
2π
θ

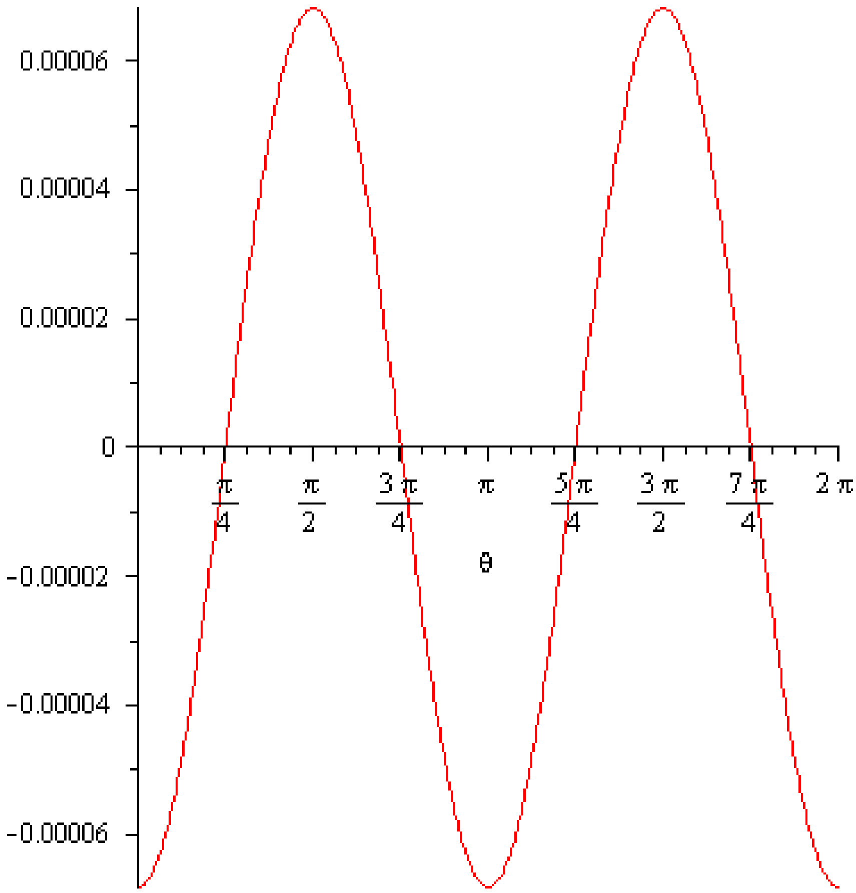
0.00006
0.00004
0.00002
0
-0.00002
-0.00004
-0.00006
π/4
π/2
3π/4
π
5π/4
3π/2
7π/4
2π
θ

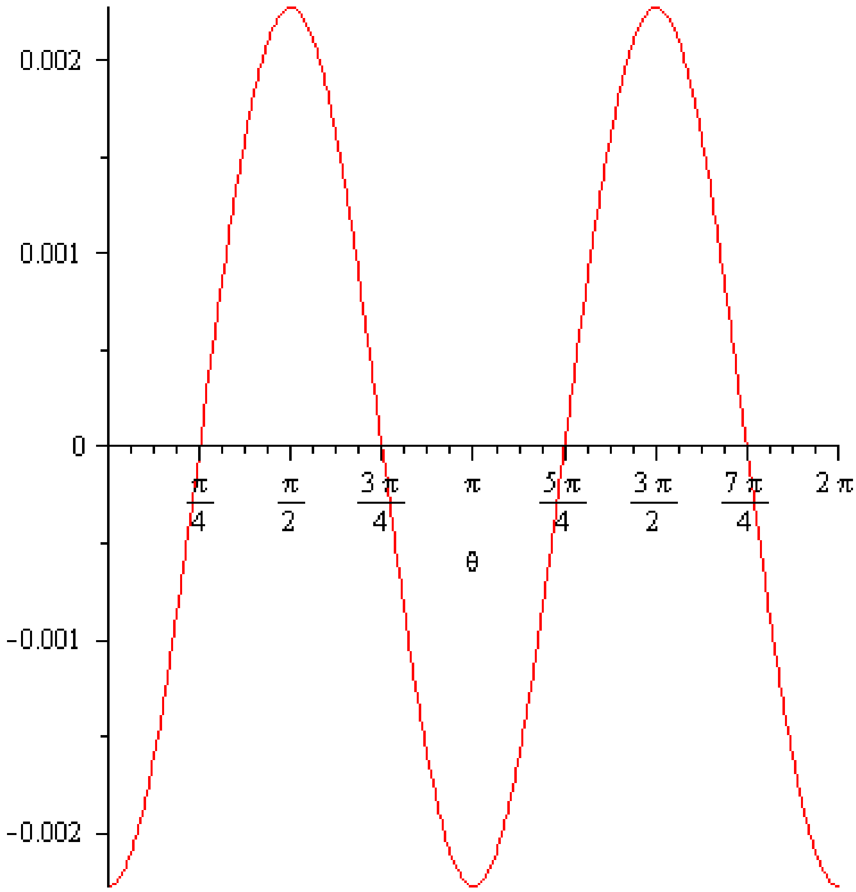

$$\theta := \frac{1}{2}\pi$$

TotalTrackLengthInMeters := 1820.4000

SingleParallelArm1 :=

$1.302341979436165305938663491473802177981823789699510^{7}$

SinglePerpendicularArm2 :=

$1.302341221664518579511309563547150321490054708427910^{7}$

TimeDiffPs := 7.577716467264273539279266518564917690812716

PhaseDiffDegrees :=

0.024551801353936246267264823520150333318233199725659

Arm1TimePs :=

$1.302341979436165305938663491473802177981823789699510^{7}$

Arm2TimePs :=

$1.302341221664518579511309563547150321490054708427910^{7}$

VacuumModeTimePs :=

$6.072200788987159910473798510301416588672153987276110^{6}$

SignalSpeedArm1 :=

$1.397789542795911592456282678834611811726434662572210^{8}$

SignalSpeedArm2 :=

$1.397790356104486950050119606494778600595682887974610^{8}$

NumberOfCyclesInArm1 :=

117.21077814925487753447971423264219601836414107296

$NumberOfCyclesInArm2 :=$
117.21070994980667215601786071924352893410492375851

$TimeDifferencePs :=$
7.577716467264273539279266518564917690812716

>

References

[1] Torr D.G. and Kolen P. In: Precision Measurements and Fun-damental Constants, Taylor, B.N. and Phillips, W.D. eds. Natl.Bur. Stand. (U.S.), Spec. Pub., 1984, 617, 675.

[2] Krisher T.P., Maleki L., Lutes G.F., Primas L.E., Logan R.T., Anderson J.D. and Will C.M. Test of the isotropy of the one-way speed of light using hydrogen-maser frequency standards.
Phys. Rev. D, 1990, v. 42, 731–734

[3] Cahill R.T. The Roland DeWitte 1991 experiment. Progress inPhysics, 2006, v. 3, 60–65.

[4] Anderson J.D., Campbell J.K., Ekelund J.E., Ellis J. and Jordan J.F. Anomalous orbital-energy changes observed during space craft flybys of Earth. Phys. Rev. Lett., 2008, v. 100, 091102.

[5] Cahill R.T. Combining NASA/JPL One-Way Optical-Fiber Light-Speed Data with Spacecraft Earth-Flyby Doppler-Shift Data to Characterise 3-Space Flow. Available from:

https://www.researchgate.net/publication/26842358_Combining_NASAJPL_One-Way_Optical-Fiber_Light-Speed_Data_with_Spacecraft_Earth-Flyby_Doppler-Shift_Data_to_Characterise_3-Space_Flow [accessed Feb 11 2023].

[6] Traill. D. The Light Timing Calculations of the Interferometer in the Quest to Detect Light Speed Anisotropy and a Case Study of the Michelson-Morley and Miller Mt Wilson Experiments.

Journal of Applied Mathematics and Physics > Vol.10 No.3, March 2022

DOI: 10.4236/jamp.2022.103055

Available from:

https://www.scirp.org/journal/paperinformation.aspx?paperid=115944 [accessed Feb 11 2023].